

# Polymer Hydrogenation in Pulsed Flow Systems with Extrusion

Alan Bussard and Kerry M. Dooley

Dept. of Chemical Engineering, Louisiana State University, Baton Rouge, LA 70803

DOI 10.1002/aic.11448

Published online February 19, 2008 in Wiley InterScience (www.interscience.wiley.com).

*The hydrogenation of poly(styrene) over a Pd/Al<sub>2</sub>O<sub>3</sub> catalyst was studied in reactors where pulsed flows are present due to both extrusion and forced pulsing. The reaction was investigated over a range of flow rates, polymer concentrations, and pulsing conditions. Observed activities were highly related to gas-to-liquid mass transfer rates predicted by a correlation for slug flow in catalyst monoliths. A reactor fed by a liquid-starved extruder is an attractive choice for hydrogenation at low polymer concentrations, where intrinsic reaction rates are approached. Higher polymer concentrations (10 wt %) lead to higher mass transfer resistances and a decrease in observed activity. But in this case forced pulsing has a greater effect on productivity; an optimum pulsing frequency was observed. Selectivity was higher and power input lower than in a stirred tank at comparable conditions. The optimal frequency is higher than those found in previous work on hydrogenations. © 2008 American Institute of Chemical Engineers AICHE J, 54: 1064–1072, 2008*

**Keywords:** reactor analysis, catalysis, polymer processing, mass transfer, extruder

## Introduction

The ability to chemically modify polymers has recently engendered increased interest as a way to economically develop new materials. With chemical modification, there is no need to develop a new process for the monomer(s), and certain structures of commercial interest are only available synthetically through polymer modification reactions. Such reactions may also improve material properties such as resistance to chemical degradation and mechanical strength. Therefore, polymer modification reactions provide another way to individually tailor polymer architectures for a specific use. One type of reaction that has been researched extensively is the modification of poly(butadiene) (PBD). Alternating double bonds in PBD allow the addition of functional groups by either homogeneous or heterogeneous catalysis.<sup>1</sup> The simplest PBD modification reaction is hydrogenation.<sup>1,2</sup> More elaborate modifications such as the synthesis of PBD polyols

are also possible, but only with careful control of the extent of backbone functionalization and the prevention of cross-linking.<sup>3</sup>

While several PBD modifications have been successful, the heterogeneously catalyzed hydrogenation of poly(styrene) (PS) to poly(vinylcyclohexane) (PVCH) (Figure 1) has proved more difficult.<sup>4–8</sup> This is because the stabilizing effect of the aromatic ring resists hydrogenation at mild reaction conditions. While PBD can be completely saturated at 343 K and 3.5 MPa, PS hydrogenation conditions typically range from 412 to 473 K at pressures of 3.5–6.9 MPa, while still requiring 8–24 h for near-complete conversion.<sup>4,6</sup> These high temperatures can also reduce molecular weight (MW) through backbone chain scission. High pressures are particularly necessary in stirred tanks because the catalyst particle is fully wetted, meaning hydrogen must always overcome gas–liquid and liquid–solid mass transfer resistances. Most literature studies have focused exclusively on processing in batch stirred tanks,<sup>4–7,9</sup> while one source has investigated the use of catalyst-coated monoliths mounted on stirrers.<sup>8</sup> Stirred tanks, where the catalyst is present in the form of a slurry, are less practical since the catalyst must be filtered from the

Correspondence concerning this article should be addressed to K. M. Dooley at dooley@lsu.edu.

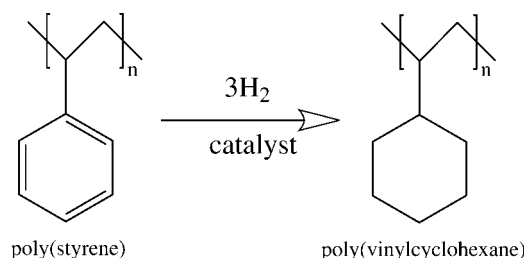


**Figure 1. Hydrogenation of poly(styrene) to poly(vinylcyclohexane).**

products post reaction. Continuous processing is also usually preferred over batch mode.

Current commercial three-phase reactors, such as packed beds operated in trickle flow mode, are ill-equipped to deal with polymer systems. As is well known, these reactors can suffer from rivulet formation and inhomogeneous residence time distributions (RTD); higher viscosity polymer solutions exacerbate these problems. A large variation in RTD can also contribute to poor reaction selectivity where the pathway is serial in nature and an intermediate product is desired.<sup>10</sup> Research to improve mass transfer rates and control surface wetting for three-phase systems has recently focused on pulsed-flow operation, where alternating gas- and liquid-rich conditions exist at the surface of a catalyst.<sup>10–15</sup> Pulsed flow can realize certain advantages of partial catalyst wetting. During the gas-rich cycle, the gas is supplied to the surface with minimal liquid film resistance. The liquid-rich cycle supplies fresh reactant, while flushing away product and providing a high rate of heat transfer. This method of deliberate unsteady-state operation has been shown to enhance reaction rates for the hydrogenation of alpha-methylstyrene (AMS) in a packed bed.<sup>14</sup> It is also believed this type of flow can enhance serial pathway selectivity by giving a more uniform RTD.<sup>10</sup> Boelhouwer et al.<sup>10</sup> noted there should be an optimal frequency for such pulsing to minimize side products, and that this optimum would be governed by the rates of heat generation and reaction. However, they also noted the inherent impracticality of pulsing trickle beds at high (beyond 1 Hz) frequencies in large (>3 m) columns where pulses would coalesce and decay unless other operating conditions, such as superficial gas velocity, were not within a narrow range.<sup>10</sup> Predicting optimal pulsing conditions (e.g., frequency, amplitude) is difficult since they are a function of reactor dimensions, operating conditions, and certain characteristics of the reaction.

Monolith reactors operated in the Taylor (slug) flow regime have also been investigated for improved three-phase reactor operation.<sup>16–19</sup> They have also shown rate enhancements for AMS hydrogenation compared with conventional stirred tanks.<sup>19</sup> Taylor flow consists of inherent pulsing behavior in monolith channels, with intermittent gas slugs. Such flow exhibits high rates of mass transfer because each liquid slug is well-mixed and the gas slugs are surrounded by only a thin liquid film, minimizing the gas diffusion length.<sup>20</sup> These reactors can also approach plug flow behavior,<sup>19</sup> thereby improving serial pathway selectivity in some hydrogenations, compared with trickle beds.<sup>19</sup> Heibel et al.<sup>21</sup> noted that increasing viscosities would give thicker films surround-

ing gas slugs, which would presumably reduce the rates of mass transfer.

Because the extension of these pulsed systems to the modification of polymers has never been realized, it would be beneficial to examine the effects of pulsed operation on a model reaction like PS hydrogenation. Extruders, commonly used for polymer melt processing, exhibit flow instabilities as a result of partial screw filling.<sup>22</sup> In this mode of operation (i.e., liquid-starved), alternating regions of gas and polymer are transported along the extruder barrel where they affect flow at the exit die (e.g., surging or spurt flow). Therefore, extrusion in gas-liquid systems also exhibits unsteady flow behavior similar to that of monoliths and pulsed trickle beds. While most researchers have tried to limit oscillatory extruder behavior because it is often detrimental to materials processing, our goal is to use this behavior to our advantage in the reaction. This paper focuses on the applicability of pulsed flows to polymer modification reactions, and on combining the inherent unsteady flow of the extrusion process with heterogeneous catalysis in a novel reactor system that can improve polymer hydrogenation.

## Experimental

### Catalyst preparation

A Pd/ $\gamma$ -Al<sub>2</sub>O<sub>3</sub> catalyst was prepared by ion exchange. Pseudoboehmite (UOP Versal V-250) was calcined at 773 K in flowing air to dehydroxylate to the  $\gamma$ -phase. A Pd(NH<sub>3</sub>)<sub>4</sub>(NO<sub>3</sub>)<sub>2</sub> solution was prepared from PdCl<sub>2</sub> by dissolving in excess aqueous ammonia and NH<sub>4</sub>NO<sub>3</sub> at a pH of 11. The Cl<sup>–</sup> was removed by contacting the solution with an ion exchange resin (IRA-400, Rohm and Haas). This solution was then mixed with the alumina at 333 K overnight. The resulting solid was filtered, dried at 353 K, then calcined at 773 K in flowing air, and finally reduced at 403 K in 10% H<sub>2</sub>/N<sub>2</sub>. The catalyst had a final Pd content of 0.5 wt % (determined by ICP-AES) after three consecutive ion exchanges, with drying, calcining, and reduction done after each exchange.

This catalyst was either washcoated on 100 cells per square inch cordierite monoliths with cylindrical channels (0.2 cm channel diameter, 1.2-cm length) or pressed into 20–35 mesh pellets. Washcoating took place from a stirred aqueous slurry, at 25 wt % solids content, with 0.1 mol L<sup>–1</sup> nitric acid added dropwise during the process to maintain the pH at 3.5–4. An acidic pH creates charge barriers that prevent the alumina particles from aggregating.<sup>23</sup> The slurry was then ball milled for 90 min to reduce the average particle size below 10  $\mu$ m. This was verified by examining the particles before and after milling by SEM. Ball-milled samples were stable for days without stirring. Dry, bare monoliths were dipped into the slurry and excess slurry removed with compressed air. As-coated monoliths were dried at 363 K, calcined at 773 K, and reduced at 403 K in 10% H<sub>2</sub>/N<sub>2</sub>. This resulted in repeatable washcoat loadings of 4 wt % at a coating thickness of 100  $\mu$ m. The final catalyst had a BET surface area of 290 m<sup>2</sup> g<sup>–1</sup> (determined using a Quantachrome AS-1) and a dispersion of 74% by H<sub>2</sub> chemisorption (determined using a Micromeritics 2700). Using the Barrett-Joyner-Halenda algorithm, the average pore size was found to be 10 nm with a full width at half maximum of 4 nm based on the desorption branch.

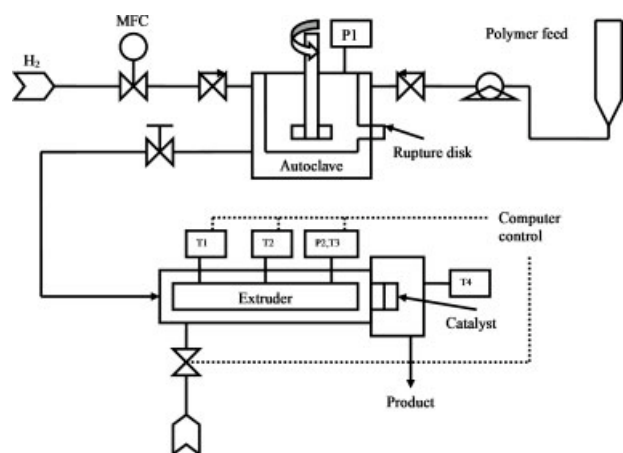


**Figure 2. Schematic of the pulsed extruder-reactor.**

### Reactor setup and procedure

The pulsed reactor was based on a research grade twin-screw extruder (Haake Rheocord 9000). A schematic of the system is shown in Figure 2. The counter-rotating screws have a  $L/D$  aspect ratio of 13. Custom-made dies housing the catalyst (packed bed or monolith) was placed at the exit of the extruder. The square die held square catalyst-coated monoliths (5.75 cm sides, 1.2-cm length), and was shaped to match the monolith dimensions. The cylindrical die (1.75 cm diameter, 15.5 cm length) held a packed bed of catalyst particles. The mean residence times were from 10 to 56 min for the monolith die and 16 and 73 min for the packed bed die. The PS (Dow Styron,  $MW_i = 230 \text{ kg mol}^{-1}$ ) was dissolved in a mixture of 10 vol % THF/cyclohexane<sup>7</sup> (cyclohexane, Sigma-Aldrich, 99+%; THF, Fisher, 99.9%) at a concentration of 2 or 10 wt %. This solution was premixed with hydrogen at high pressures in a stirred tank before both phases were fed to the extruder at the screw head. The screw speed was held constant at 10 rpm. Heating bands around the barrel and die provided temperature control. A photocell positioned at the die exit recorded flow instabilities in the form of voltage changes. In order to better control pulse frequency, a computer-controlled solenoid valve was attached to the extruder barrel so that additional hydrogen could be injected into the system at user-defined intervals. This mode of operation is referred to as forced pulsing. The polymer solution was fed by a piston pump (Eldex B-100-S-4) such that the level in the stirred tank was constant. Hydrogen flow into the system was recorded by mass flow controller (Brooks 5850C). When not in operation, the reactor was left under 0.34 MPa hydrogen partial pressure to keep the Pd catalyst in the reduced state.

Several experiments using a high pressure stirred tank (Autoclave Engineers Zipperclave, 500 cm<sup>3</sup>) reactor were also done for comparison purposes. The impeller was a three-bladed marine propeller with no gas sparger or baffles. The catalyst was present as either a powder or a catalyst-coated monolith placed at the bottom of the reactor. The stirred tank was operated at 2600 rpm and 423–453 K with 2 and 10 wt % PS solutions. The reactor could be intermittently sampled through a dip-tube. This reactor was also maintained under hydrogen purge between runs to maintain the catalyst's reduced state.

Conversion was determined using a Jasco V-570 UV–vis spectrometer, by monitoring the decrease in absorbance of the aromatic peak at 262 nm of samples diluted in chloroform (Mallinckrodt, 99.9%). This absorbance was correlated to the conversion of aromatic groups using a linear calibration developed from <sup>1</sup>H NMR data on samples reacted to various conversions in a stirred tank. The NMR data were related to aromatic group conversion according to Gehlsen et al.<sup>7</sup> The reactor was operated in single-pass mode with a limited amount of catalyst, such that PS conversions were low (2–7%). Polymer MW changes were monitored by performing intrinsic viscosity measurements on product samples dissolved in toluene based on standard Mark-Houwink constants for polystyrene.<sup>24</sup> Selected liquid samples with the polymers removed through distillation were analyzed by GC-MS (HP 5972). Key extruder/reactor measurements were interfaced to LabView<sup>®</sup> through an MIO-16E data acquisition card (National Instruments).

## Results and Discussion

### Flow behavior in the pulsed reactor

The range of two-phase flow for PS hydrogenation in the extruder-fed reactor was from  $G/L$  (ratio of volumetric flow rates at reaction conditions) of 0.5 at 2.0 MPa to  $G/L = 1.2$  at 3.5 MPa. Below 2.0 MPa, there were periods of little to no gas exiting the extruder. Above 3.5 MPa,  $G/L$  did not significantly increase. The range of superficial gas and liquid velocities ( $u_G$  and  $u_L$ ) explored in this study was 1–16 cm/h, calculated using the channel diameter. To our knowledge, no previous work to develop flow regime maps at such low flow rates and with viscous polymeric systems has been published. However, extrapolating data from flow maps in similarly sized circular channels indicates operation in the slug flow regime,<sup>25</sup> which is confirmed by experimental data from the photocell. Figure 3 shows the time evolution of gas holdup for the two phase flow exiting the die as recorded by the photocell. The flow is discontinuous with alternating gas (low photocell voltage) and liquid slugs (high photocell voltage), characteristic of a liquid-starved extruder.<sup>22</sup> These regions of discontinuous gas- and liquid-rich flow arise within the screw flights and persist through the monolith channels inside the die. Taylor (slug) flow is usually the desired mode of operation for three-phase monolith reactors, when reactions are highly gas mass-transfer limited.

Figure 3a shows the natural pulsing behavior of the reactor while Figure 3(b) shows the effects of forced pulsing at 0.1 Hz. Forced pulsing resulted in periodic spikes in gas flow in the monolith. These large gas slugs are superimposed on the pulses inherent to the system. Spikes in gas flow appear as lower voltages of ~20 s duration, centered around 40 s and 90 s in Figure 3(b). The exit age distribution of these spikes could not be controlled by varying the inlet pulsing frequencies from 0.1 to 0.5 Hz for either the 2 or 10 wt % PS solutions. Other attempts to control the exit distribution of these spikes by varying flow rates, pressures, and screw speed were also unsuccessful. Pulsing at 0.5 Hz did result in longer gas spikes exiting the extruder, but nevertheless the average pulse frequency at the exit was similar to that for 0.1 Hz and for unforced operation (Table 1). In other words, the impact

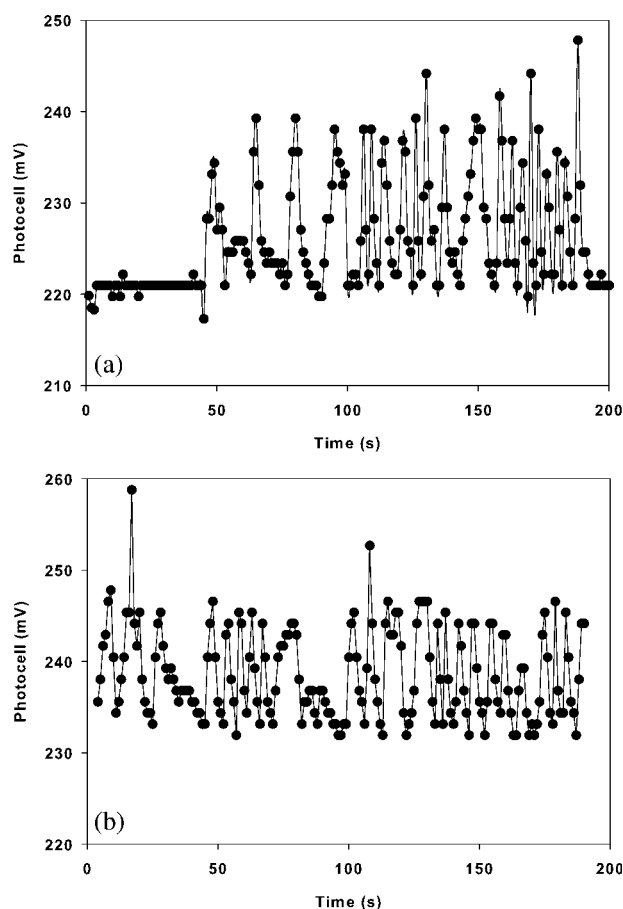


**Figure 3. Alternating gas/liquid flow from catalyst monolith operated under: (a) unforced (natural) pulsing conditions, with flow initiated at 45 s; (b) forced pulsing, 0.1 Hz.**

Voltages near 220 mV in (a) and 230 mV in (b) represent slugs of gas; voltages near 240 mV in (a) and 250 mV in (b) represent slugs of liquid.

on the average frequency of occasional large gas slugs was small, but the average amplitude of the exit pulses did decrease as the forced pulsing frequency increased (Table 1), indicating more foam. No changes in the die or barrel pressure greater than 25 kPa were measured in any experiment, either with natural or forced pulsing. The inability to control the average exit pulse frequency is most likely due to gas backmixing in the extruder barrel and bubble coalescence prior to the die exit. Problems associated with controlling pulse behavior due to coalescence have also been reported in previous work on pulsed trickle beds.<sup>12</sup>

**Table 1. Average Pulse Characteristics for Forced and Unforced Pulsing**

Forced Oscillation Frequency (Hz)	Average Outlet Frequency (Hz)	Average Amplitude (mV)
None	0.13	8
0.1	0.14	6.5
0.5	0.16	2.5

## Hydrogenation studies

The only observed product was hydrogenated PS (PVCH). Previous work<sup>5</sup> has shown PS hydrogenation over Pd catalysts to be first order in aromatic concentration ( $C_A$ ) and zero order in hydrogen concentration ( $C_H$ ) for  $\leq 3$  wt % PS in stirred tanks at greater than 3.0 MPa. At high rates of agitation (e.g., >2000 rpm) there were no significant external liquid, intraparticle, or gas-phase concentration gradients. Below 3.0 MPa, the dependence on hydrogen concentration was linear.<sup>5</sup> Using these results, observed rate constants for the reactor at lower pressures were determined by modeling the system mass balance as a plug flow reactor with first-order kinetics dependencies for both reactants (Eq. 1), using the reaction stoichiometry of Figure 1. In the limit of zero resistances to mass transfer, the  $k'_{\text{obs}}$  in Eq. 1 is the intrinsic rate constant for the reaction. From  $k'_{\text{obs}}$  a pseudo-first order (in aromatic group) rate constant ( $k_{\text{obs}}$ ) was calculated (Eq. 2) by multiplying by a reference hydrogen concentration  $C_{Hr}$  (0.238 mol  $H_2$ /L, the solubility in cyclohexane at 3.4 MPa and 453 K). In this manner we obtained a  $k_{\text{obs}}$  that was independent of  $H_2$  pressure. Both  $C_{Hr}$  and the feed concentration  $C_{Ho}$  were obtained using the Henry's Law coefficient for hydrogen solubility in cyclohexane,<sup>26</sup> thereby assuming that the small amounts of THF and PS did not significantly impact the solubility of  $H_2$  in the solvent.

$$W = \frac{v_o}{k'_{\text{obs}}} \int_0^X \frac{1}{(C_{Ho} - 3XC_{Ao})(1 - X)} dX \quad (1)$$

$$r_{\text{obs}} = k'_{\text{obs}} C_A C_H; \quad k_{\text{obs}} = k'_{\text{obs}} C_{Hr} \quad (2)$$

The pulsed reactor was operated at lower pressures and power/volume ( $P/V$ ) ratios than the agitated vessel, but gave similar results for  $k_{\text{obs}}$ . For the agitated vessel at >3.0 MPa,  $k_{\text{obs}}$  was computed using a batch reactor mass balance, with kinetics dependencies of first order in aromatic concentration and zero order in hydrogen. This method allowed rough quantitative comparisons between the two modes of operation.

To investigate the effects of washcoating the catalyst on a ceramic monolith, reactions were performed in the agitated vessel using the catalyst present as either a powder ground to 100–120 mesh or as a washcoated monolith at the bottom of the stirred tank. The results of these runs are summarized in Table 2. At temperatures of both 423 and 453 K,  $k_{\text{obs}}$  was

**Table 2. Agitated Vessel Experiments for Powdered and Monolith-Supported Catalysts\***

Run	Pressure (MPa)	Temperature (K)	$k_{\text{obs}}$ ( $LS^{-1} g_{Pd}^{-1}$ )
powder_1	3.4	423	$3.1 \times 10^{-5}$
monolith_1	3.4	453	$2.9 \times 10^{-5}$
powder_2	3.4	453	$9.0 \times 10^{-5}$
monolith_2	3.4	453	$9.1 \times 10^{-5}$
powder_3 <sup>†</sup>	3.4	453	$1.1 \times 10^{-4}$
powder_4 <sup>‡</sup>	3.4	453	$5.4 \times 10^{-5}$

\*All runs at 2600 rpm, 2 wt % PS unless otherwise noted; the numbers (powder\_1, etc.) refer to run numbers.

<sup>†</sup>10 wt % PS feed.

<sup>‡</sup>1000 rpm.

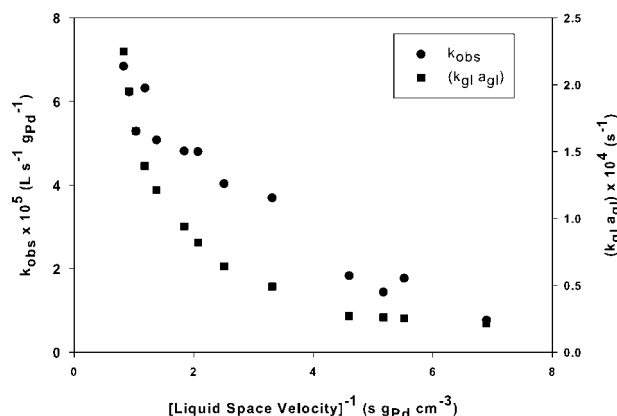


**Figure 4. Hydrogenation of 2 wt % PS, 453 K, 3.13 MPa, no forced pulsing, G/L (volumetric)  $\sim 1.2$ .**

independent of catalyst form, proving the washcoated monolith is chemically identical to the powdered version. Increasing the hydrogen partial pressure to 5.5 MPa did not result in a higher rate of reaction, indicating that the  $k_{\text{obs}}$  values at high rpm in Table 2 are representative of the intrinsic kinetics at their respective conditions, and that these kinetics are indeed zero-order in  $\text{H}_2$  at high pressures. Xu et al.<sup>5</sup> reported intrinsic activities of  $3.2 \times 10^{-5} \text{ L s}^{-1} \text{ g}_{\text{Pd}}^{-1}$  at 423 K and  $1.4 \times 10^{-4} \text{ L s}^{-1} \text{ g}_{\text{Pd}}^{-1}$  at 453 K for a 5 wt % Pd/BaSO<sub>4</sub> catalyst. These values are similar to those reported in Table 2 for both powdered and monolith-supported catalysts. However, a direct comparison between the intrinsic activities of the catalysts used by Xu et al. and this study is difficult because of the differences in catalytic properties (e.g., Pd dispersion) as well as the effects of the solvent (Xu et al. used decahydronaphthalene).

To determine if intraparticle gradients were present, Weisz-Prater moduli<sup>27</sup> ( $C_{\text{WP}}$ ) were computed based on the highest observed rates for both the monolith-supported and powdered catalysts at 2 wt % PS. The diffusivity of  $\text{H}_2$  was calculated using the Wilke-Chang correlation,<sup>28</sup> and from this an effective diffusivity was obtained using average catalyst properties. The hydrogen solubility was obtained from the literature.<sup>26</sup> The modulus for 2 wt % PS was 0.02 for the powdered catalyst and 0.03 for the monolith-supported catalyst. This confirms that for the 2 wt % PS system, pore diffusion is neither limiting nor significant.

Figure 4 shows results for the hydrogenation of a 2 wt % PS solution for a monolith die, no forced pulsing. Also plotted is a correlation for the gas to liquid mass transfer coefficient times the interfacial area per volume ( $k_{\text{gl}}a_{\text{gl}}$ ) for slug flow in monoliths. The  $\text{H}_2$  concentration gradient in the liquid multiplied by  $k_{\text{gl}}a_{\text{gl}}$  is the observed rate ( $r_{\text{obs}}$ ). The correlation for  $k_{\text{gl}}a_{\text{gl}}$  is shown as Eqs. 3<sup>29</sup> and 4.<sup>20</sup> Equation 4 adjusts the methane-water coefficient to the present system.  $L_{\text{slug}}$  was approximated as the length of a monolith channel, although its magnitude will not affect the shape of the curve. Higher two-phase velocities ( $u_{\text{tp}} = u_{\text{L}} + u_{\text{G}}$ ) through the die result in faster mass transfer from gas to liquid, and this is closely reflected in the observed rate of reaction under unforced conditions (Figure 4); the results confirm that the

reaction is gas mass-transfer limited at these lower pressure conditions. At high liquid space velocities ( $0.5\text{--}1.25 \text{ cm}^3 \text{ s}^{-1} \text{ g}_{\text{Pd}}^{-1}$ ) the observed rate constants are within 30% of the intrinsic rate constant at this temperature ( $\sim 9 \times 10^{-5} \text{ L s}^{-1} \text{ g}_{\text{Pd}}^{-1}$ , see Table 2).

$$(k_{\text{gl}}a_{\text{gl}})_{\text{M}} = \frac{0.133 u_{\text{tp}}^{1.2}}{L_{\text{slug}}^{0.5}} \quad (3)$$

$$(k_{\text{gl}}a_{\text{gl}}) = (k_{\text{gl}}a_{\text{gl}})_{\text{M}} \left( \frac{D_{\text{H}}}{D_{\text{M}}} \right)^{0.5} \quad (4)$$

The added effect of forced pulsing at 0.1 Hz on PS hydrogenation is shown in Figure 5. Because the  $G/L$  ratio and reactor pressure could not be varied independently in the pulsed reactor, and because the  $\text{H}_2$  pressure dependence on the kinetics was known, the pressure for the forced pulsing experiments was decreased somewhat to keep the  $G/L$  volumetric ratio the same as in the unforced experiments. In this manner, any changes in  $k_{\text{obs}}$  could be attributed to the effects of the pulsing itself. When the pressure differences are taken into account assuming first-order kinetics in  $\text{H}_2$ , the observed rates for either natural or forced pulsing are virtually identical (compare Figures 4 and 5). In other words, for a low viscosity (zero-shear viscosities of 2.2 mPa·s for 2 wt % PS, 37.2 mPa·s for 10 wt % PS, at 296 K) 2 wt % PS solution, the inherent, natural oscillations caused by the extruder are sufficient to give reaction rates near those of an intensely agitated tank. The maximum  $k_{\text{obs}}$  for a 2 wt % PS solution is  $\sim 7 \times 10^{-5} \text{ L s}^{-1} \text{ g}_{\text{Pd}}^{-1}$  at high superficial velocities, where the resistance to gas-liquid mass transfer is minimized. Again,  $k_{\text{obs}}$  scales well with the computed ( $k_{\text{gl}}a_{\text{gl}}$ ) for slug flow, indicating that gas-to-liquid mass transfer is still limiting. Attempts to increase the superficial velocities further to eliminate the remaining transport resistances resulted in flow instabilities and a transition to a purely foam-type flow, accompanied by a decrease in  $k_{\text{obs}}$ . We conclude that there is a well-defined optimal superficial velocity giving the hydrodynamic environment that minimizes resistance to external mass transfer in the monolith-supported catalyst.

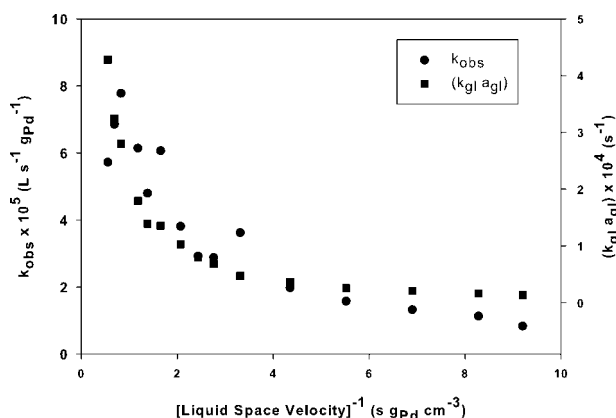


**Figure 5. Hydrogenation of 2 wt % PS, 453 K, 2.65 MPa, 0.1 Hz forced pulsing, G/L (volumetric)  $\sim 1.2$ .**

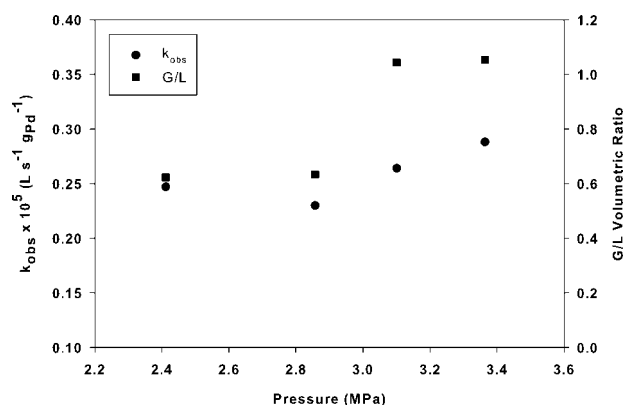


**Figure 6. Hydrogenation of 10 wt % PS, 453 K, no forced pulsing, monolith die, inverse liquid space velocity of  $13.8 \text{ s g}_{\text{Pd}} \text{ cm}^{-3}$ .**

Figure 6 shows the effect on the reaction of varying the system pressure for a 10 wt % PS feed. As seen, the pseudo first-order rate constants for the pulsed reactor vary slightly over the pressure range 2.4–3.4 MPa. This variation can be explained by concomitant variation in  $G/L$ , which increases noticeably at  $>3.0$  MPa. A higher  $G/L$  results in thinner liquid films surrounding the gas slugs, and so often enhanced gas–solid mass transfer. Changes in  $G/L$  of this magnitude typically have minimal effects for inviscid Newtonian systems.<sup>21</sup> However, the effects of  $G/L$  here are greater, as these solutions are shear-thinning, and therefore more affected by the shearing behavior of the liquid film.

To accurately measure  $k_{\text{obs}}$  for more concentrated (and less reactive) feeds, more catalyst was required, and so for reasons of synthetic ease we switched from a monolith to particulate catalyst, present as a packed bed. The catalyst was still contained in the die of the extruder, and other operating conditions were also unchanged. The exit pulse characteristics described in Table 1 were also maintained. In Figure 7, we show  $k_{\text{obs}}$  for 10 wt % feeds, for both unforced and

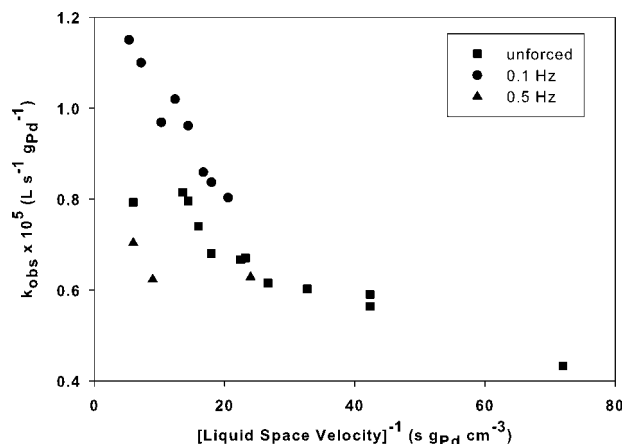


**Figure 7. Hydrogenation of 10 wt % PS at 453 K, packed bed die.**

Pressures are 3.24 MPa for unforced pulsing, 2.65 MPa for 0.1 and 0.5 Hz forced pulsing.

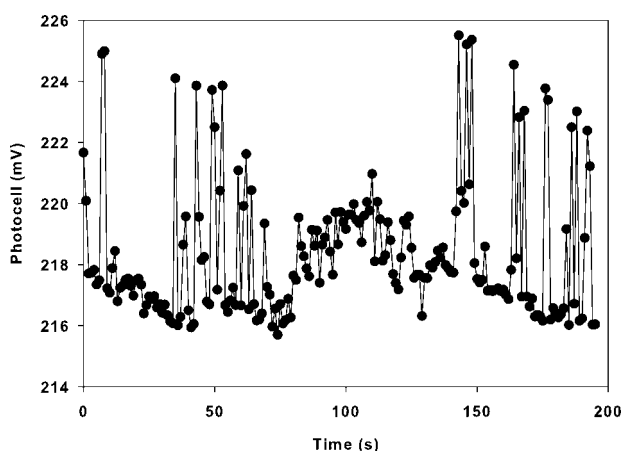


**Figure 8. Gas/liquid behavior at die exit for 0.5 Hz forced pulsing, 10 wt % PS, packed bed die.**

Voltagages near 216 mV represent slugs of gas; voltagages near 225 mV represent slugs of liquid.

forced (0.1 and 0.5 Hz) pulsing modes. The data again show an increase in  $k_{\text{obs}}$  with liquid flow rate. However, the observed rates for the 10 wt % PS solutions are approximately one order of magnitude less than for the 2 wt % solutions, findings consistent with much greater diffusional resistance associated with higher viscosity. The 0.5 Hz data show a decrease in  $k_{\text{obs}}$  compared with both the unforced and 0.1 Hz runs. This decrease can be attributed to the longer period of the flow instabilities, consisting of intervals of large gas slugs and almost dry catalyst (see Figure 8). Clearly, the highly liquid-starved condition over an extended period is not conducive to macromolecular hydrogenation. In Figure 8, note the extended periods of the large gas slugs at 0.5 Hz forced pulsing. For 0.1 Hz forced pulsing,  $G/L$  of 1.2,  $k_{\text{obs}}$  computed by Eqs. 1 and 2 is 20–40% higher than for unforced operation, depending on the space velocity (Figure 7). This indicates that forced pulsing can either increase or decrease the observed rate constant for more viscous and shear-thinning feeds, depending upon the frequency and the space velocity. For low frequency and high space velocity, there is a definite increase in  $k_{\text{obs}}$ .

Note that increasing the PS concentration from 2 to 10 wt % in the agitated vessel reaction experiments (Table 2) left  $k_{\text{obs}}$  virtually unchanged, while similar experiments in the pulsed reactor resulted in a nine-fold decrease. This highlights the important role of solution viscosity on the mass transfer. While the natural or forced pulsing of the extruder-fed reactor can affect the wetting behavior by alternating mostly gas and mostly liquid slugs, it has less effect on viscosity, because the average shear rates for the continuous reactor experiments are low. However, in the agitated vessel at high stirrer speeds, the shear rates are large near the agitator, resulting in a low viscosity for the shear-thinning polymer solution. We examined the viscosity of the 10 wt % solution at ambient conditions in a cone and plate viscometer, and found that shear rates  $>4 \text{ s}^{-1}$  resulted in approximately a 90% reduction in viscosity from the zero-shear value. At the high rpm conditions of Table 2, the shear rate at the tip of the agitator was greater than  $500 \text{ s}^{-1}$ . Assuming no gas in the packed bed, the shear

rates here were only 0.03–0.07 s<sup>-1</sup>. Therefore, it is not surprising that the agitated vessel experiments showed no effect of feed concentration. Since the particles used in the packed bed were necessarily larger than the powdered catalyst in the stirred tank experiments (to avoid large pressure drops), the Weisz-Prater moduli  $C_{WP}$  were also computed for 10 wt % PS feed. In the stirred tank with powdered catalyst,  $C_{WP}$  was 0.07, indicating negligible pore diffusion resistance. For the packed bed system,  $C_{WP}$  was 0.21, suggesting modest intra-particle gradients. Therefore, the Thiele modulus ( $\phi$ ) and effectiveness factor ( $\eta$ ) were computed assuming spherical pellet geometry, giving  $\eta = 0.93$  for the packed bed catalyst at 10 wt % PS. So the reaction was still largely limited by the resistance to gas–liquid mass transfer, as has been well documented for this system.

To examine reactor effects on the selectivity of hydrogenation, certain product samples from the stirred tank and pulsed reactor experiments were analyzed by intrinsic viscosity measurements. No samples (natural or forced pulsing) from the extruder-fed reactor showed any decrease in MW at the conversions obtained in this study. However, the stirred tank samples did show some hydrocracking at similar conversions. For instance, the average MW was reduced from 230 to 200 kg mol<sup>-1</sup> at a PS conversion of 6% in the stirred tank. This result is significant because it demonstrates there is a clear advantage in using a structured catalyst with alternating gas- and liquid-rich conditions at the surface. Selectivity enhancements have also been found previously for catalyst monoliths operated in slug flow when applied to low MW hydrogenations.<sup>30,31</sup> These enhancements are presumed to arise from more uniform residence times on the catalyst surface (for the polymer) and more plug flow-like behavior. The present work shows that these selectivity enhancements can be extended to polymer systems as well. The natural pulsing behavior of the extruder system is sufficient to “flush” PS from the surface of the catalyst before a chain scission event can occur, because we found that the longer gas slugs arising from forced pulsing did not give any further selectivity enhancements.

A perhaps more illuminating way to compare stirred tank performance to the pulsed reactor is by examining the power input to each system. The power input ( $P$ ) to the stirred tank was calculated using Eq. 5<sup>32</sup> where  $N_o$  is a constant depending on the impeller shape (0.8 for a three-bladed marine propeller).<sup>32</sup>

$$P = N_o \rho N^3 D^5 \quad (5)$$

The power input for the extruder-fed reactor was approximated by multiplying the volumetric flow rate by the pressure drop across the die. Calculations of the power input due to the pulsing were estimated from Eq. 6<sup>33</sup> where  $L$  is the length of the monolith and  $\omega$  represents the pulsing frequency. This power input term was negligible compared with the power input due to the pressure drop, for all runs.

$$P = \frac{1}{2} \rho L^2 \omega^3 V \quad (6)$$

Dividing the input power by the respective liquid reactor volumes gave power per unit volume ( $P/V$ ), with the result

that even for the extruder-fed reactor operating at its highest flow rate, with a 2 wt % PS solution its input  $P/V$  ( $1.2 \times 10^4$  W/m<sup>3</sup>) is only 16% of the stirred tank value at 2000 rpm. For a 10 wt % PS solution in the packed bed die,  $P/V$  is only 5% of the stirred tank value at 2000 rpm. The agitator speed required to attain negligible external mass transfer gradients at low PS concentration in typical autoclaves is ~2000 rpm, based on our own and others' results.<sup>5</sup> Note that at lower speeds  $k_{obs}$  is reduced substantially (last entry, Table 2). So we can conclude that not only can a reactor with extrusion-generated pulses approach the  $k_{obs}$  of a stirred tank for solutions of low to moderate polymer concentration, with better selectivity, but that this system also requires a lower input  $P/V$  at otherwise comparable conditions.

It is also instructive to compare the optimal pulsing frequency of the extruder system to other pulsed reactors (trickle beds), and with correlations that have been developed for finding optimal frequencies based on hydrodynamic models. The pulsed trickle bed literature on the hydrogenation of AMS over a similar Pd catalyst showed that the optimum condition depends on liquid holdup, gas superficial velocity, reaction rate and heat transfer requirements.<sup>14</sup> For this reaction, very low frequencies (~0.002 Hz)<sup>8,14</sup> were observed as optimal in pulsed trickle beds. However, other reactions have been shown to benefit from faster pulsing frequencies. For instance, the hydrogenation of 2-ethylanthraquinones over a similar Pd catalyst in a pulsed trickle bed showed an optimum at 0.01–0.02 Hz.<sup>34</sup> For the case of the extruder-fed reactor, the optimum forced pulse frequency appears to be higher (~0.1 Hz) for the PS system. PS hydrogenation is kinetically much slower than AMS hydrogenation, and slower than anthraquinone hydrogenation, since an aromatic ring is being hydrogenated vs. an unsaturated ring substituent. This suggests that as the reaction becomes kinetically more difficult, a faster pulsing frequency is advantageous. This may be because for an “easy” hydrogenation like AMS, the need for a high fugacity of adsorbed hydrogen atoms is less. The effects of surface tension may also play an important role in determining optimal pulsing conditions. Haure et al. showed that the application of water pulses to remove oxidized SO<sub>2</sub> as H<sub>2</sub>SO<sub>4</sub> from activated carbon benefited from a pulsing frequency of 0.008 Hz, but pulsing at much lower frequencies (~3 × 10<sup>-4</sup> Hz) was not effective.<sup>35</sup>

Previous work<sup>36</sup> has shown that the onset of unstable operation and thus optimal pulsing frequency for gas–liquid systems could be predicted based on the Benjamin-Ursell bubble stability theory for an inviscid solution.<sup>37</sup> This theory states that the stability is governed by Mathieu equations:

$$\frac{d^2 a_m}{dT^2} + [p_m - 2q_m(\cos(2T))]a_m = 0 \quad (7)$$

$$p_m = \left( \frac{4k_m \tanh(k_m L)}{\omega^2} \right) \left( g + \frac{k_m^2 \sigma}{\rho} \right) \quad (8)$$

$$q_m = 2k_m A \tanh(k_m L) \quad (9)$$

where, subscript  $m$  represents the  $m$ th zero of the derivative of the  $l$ th order Bessel function based on zero velocity at the channel wall.

**Table 3. Prediction of Instability Onset from Benjamin-Ursell Theory**

Die Type	Forced Pulsing (Hz)	Frequency Onset of Instability (Hz)
Monolith	N/A	92
Monolith	0.1	64
Packed bed	N/A	292
Packed bed	0.1	92
Packed bed	0.5	126

The Benjamin-Ursell theory was applied to the extruder system by solving Eqs. 8 and 9 for the frequencies leading to bubble instability. Physical values for density and surface tension were taken from simulations performed in HYSYS<sup>®</sup> 2.2 for the liquid mixture at reaction conditions. Since the forcing amplitude from previous work was based on mechanical vibrations, while the pulsing in the extruder die arose from a periodic gas flow, the derivation of pulsing amplitude was necessarily modified. The amplitudes (length of the gas slugs) inside the monolith and the packed bed were calculated from the photocell data. The pulse amplitudes were computed from the observed gas flow rate during individual gas slugs, divided by the effective diameter and multiplied by the time it took a slug to exit the die [e.g., see Figure 3(b)]. In the monolith die, this gave amplitudes of 0.01 and 0.27 cm for natural pulsing and 0.1 Hz forced pulsing, respectively. In the packed bed die, the amplitudes were 0.02, 0.4, and 0.8 cm for natural pulsing, 0.1 Hz, and 0.5 Hz forced pulsing, respectively.

Calculating the onset of instability based on  $m = 4$  and  $l = 1$ , which have been shown to provide good fits to experimental data from bubble columns for the air–water system,<sup>36</sup> gives the results shown in Table 3. The predicted onset of instability according to Benjamin-Ursell theory occurs at much higher frequencies than what we observed as optimal in the monolith die for 10 wt % PS. Other  $m$  values (1–4) for  $l$  values of 0 or 1 give similar results. This shows that the effects of pulsing on  $k_{\text{obs}}$  in solid-catalyzed systems do not arise from the onset of bubble instability. These findings also confirm the assumption, based on available data in both trickle bed and extruder-fed systems, that the wetting behavior controls the overall rate of the process. An additional complication is that Benjamin-Ursell theory was developed for large columns of free-standing liquid (i.e., bubble columns) and does not take into account secondary forces such as viscous effects. Knopf et al.<sup>36</sup> have shown that for low viscosity bubble columns, pulsing does not appreciably enhance the rates of mass transfer except at the critical frequencies leading to bubble instability, as predicted by Benjamin-Ursell theory. But clearly such considerations have little applicability to solid-catalyzed systems, whether present as monoliths or packed beds.

## Conclusions

Reactors based on pulsed flow generated by an extruder are an attractive alternative to agitated vessels for three-phase polymer modification reactions, especially at low to moderate polymer concentrations. In addition to offering the advantages of continuous processing with no catalyst separation requirement, the extruder-fed reactor can reduce the input

power/volume requirement compared with an agitated vessel, while exhibiting comparable productivity and a higher hydrogenation selectivity. For PS hydrogenation in the pulsed reactor, observed rates are highly dependent upon gas–liquid mass transfer rates. As the solution viscosity increases with increased concentration of polymer, the observed rates do decrease, although the pulse hydrodynamics remain similar.

For PS hydrogenation there is an optimal pulsing frequency, one especially observable with more concentrated solutions. The pulsing frequency regulates the liquid wetting distribution—higher frequencies leading to more foam—like behavior and decreased pulse amplitudes in the reactor. At low polymer concentrations, the pulsing frequency inherent in a liquid-starved extruder is sufficient to give an optimal wetting distribution, to the extent that even the maximum productivity of a stirred tank is approached. When processing higher concentrations of polymer, reaction productivity benefits from forced pulsing at a specific frequency, resulting in longer periods of gas-rich flow over the catalyst. However, an extension of the hydrodynamic theory that predicts high optimal pulsing frequencies for bulk liquid–gas systems is not applicable to confined polymer systems, as studied here. Also, accurately controlling the die exit behavior of the forced pulses is made difficult because of the pulse coalescence, with the result that frequencies higher than optimal significantly decrease the observed rates of reaction due to liquid starvation of the catalyst.

Compared to previous work on pulsed trickle beds for kinetically facile hydrogenations, this work shows the importance of increased pulsing frequency for a difficult gas–liquid reaction, one that is more sensitive to the concentration of adsorbed hydrogen.

## Acknowledgments

We thank NSF-IGERT (grant DGE-9987603), NASA (grant NNC06AA18A), and the Donald W. Clayton Engineering Endowment for funding this work, and Kenneth Gumpert for experimental assistance.

## Notation

- $a_m$  = surface fluid amplitude (cm)
- $A$  = forcing amplitude (cm)
- $C_{\text{Ao}}$  = initial concentration of aromatic (mol L<sup>-1</sup>)
- $C_{\text{Ho}}$  = initial concentration of hydrogen (mol L<sup>-1</sup>)
- $C_{\text{Hr}}$  = reference concentration of hydrogen (mol L<sup>-1</sup>)
- $D$  = diameter of impeller (cm)
- $D_{\text{H}}$  = diffusivity of hydrogen (cm<sup>2</sup> s<sup>-1</sup>)
- $D_{\text{M}}$  = diffusivity of methane (cm<sup>2</sup> s<sup>-1</sup>)
- $g$  = gravitational constant (cm s<sup>-2</sup>)
- $(k_{\text{gl}}a_{\text{gl}})$  = hydrogen gas to liquid mass transfer coefficient times interfacial area per volume (s<sup>-1</sup>)
- $(k_{\text{gl}}a_{\text{gl}})_{\text{M}}$  = methane gas to liquid mass transfer coefficient times interfacial area per volume (s<sup>-1</sup>)
- $k_m$  = characteristic eigenvalue (dimensionless)
- $k_{\text{obs}}$  = first order observed rate constant,  $\frac{L}{\text{sgpd}}$
- $k'_{\text{obs}}$  = second order observed rate constant,  $\frac{L^2}{\text{sgpdmol}}$
- $L$  = length of monolith or catalyst bed (cm)
- $L_{\text{slug}}$  = length of a liquid slug (cm)
- $N$  = revolutions per second (s<sup>-1</sup>)
- $N_o$  = impeller constant (dimensionless)
- $P$  = power input (W)
- $p_m$  = as in Eq. 8 (dimensionless)
- $q_m$  = as in Eq. 9 (dimensionless)
- $r_{\text{obs}}$  = observed rate of reaction,  $\frac{\text{mol}}{Ls}$
- $T$  = dimensionless time =  $\omega t/2$  (dimensionless)



$u_G$  = superficial gas velocity ( $\text{cm s}^{-1}$ )  
 $u_L$  = superficial liquid velocity ( $\text{cm s}^{-1}$ )  
 $u_{TP}$  = two phase velocity ( $u_G + u_L$ ) ( $\text{cm s}^{-1}$ )  
 $V$  = volume of liquid ( $\text{cm}^3$ )  
 $v_o$  = liquid volumetric flow rate ( $\text{L s}^{-1}$ )  
 $W$  = mass of Pd (g)  
 $X$  = fractional conversion of aromatics (dimensionless)

### Greek letters

$\rho$  = liquid density ( $\text{g cm}^{-3}$ )  
 $\omega$  = frequency ( $\text{rad s}^{-1}$ )  
 $\sigma$  = surface tension ( $\text{N m}^{-1}$ )

### Literature Cited

- McGrath MP, Sall ED, Tremont SJ. Functionalization of polymers by metal-mediated processes. *Chem Rev.* 1995;95:381–398.
- McManus NT, Rempel GL. Chemical modification of polymers—catalytic-hydrogenation and related reactions. *J Macromol Sci Rev Macromol Chem Phys C* 1995;35:239–285.
- McGrath MP, Sall ED, Forster D, Tremont SJ, Sendjarevic A, Sendjarevic V, Primer D, Jiang J, Iyer K, Klempner D, Frisch KC. Novel polymeric alcohols by controlled catalytic polymer functionalization. *J Appl Polym Sci.* 1995;56:533–543.
- Hucul DA, Hahn SF. Catalytic hydrogenation of polystyrene. *Adv Mater.* 2000;12:1855–1858.
- Xu DW, Carbonell RG, Kiserow DJ, Roberts GW. Kinetic and transport processes in the heterogeneous catalytic hydrogenation of polystyrene. *Ind Eng Chem Res.* 2003;42:3509–3515.
- Gehlsen MD, Bates FS. Heterogeneous catalytic-hydrogenation of poly(styrene)—thermodynamics of poly(vinylcyclohexane) containing diblock copolymers. *Macromolecules* 1993;26:4122–4127.
- Gehlsen MD, Weimann PA, Bates FS, Harville S, Mays JW, Wignall GD. Synthesis and characterization of poly(vinylcyclohexane) derivatives. *J Polym Sci Part B: Polym Phys.* 1995;33:1527–1536.
- Lange R, Hanika J, Stradiotto D, Hudgins RR, Silveston PL. Investigations of periodically operated trickle-bed reactors. *Chem Eng Sci.* 1994;49:5615–5621.
- Soga K, Nakatani H, Shiono T. Preparation and characterization of syndiotactic poly(vinylcyclohexane). *Macromolecules* 1989;22:1499–1500.
- Boelhouwer JG, Piepers HW, Drinkenburg AAH. Liquid-induced pulsing flow in trickle-bed reactors. *Chem Eng Sci.* 2002;57:3387–3399.
- Boelhouwer JG, Piepers HW, Drinkenburg AAH. Enlargement of the pulsing flow regime by periodic operation of a trickle-bed reactor. *Chem Eng Sci.* 1999;54:4661–4667.
- Boelhouwer JG, Piepers HW, Drinkenburg AAH. Nature and characteristics of pulsing flow in trickle-bed reactors. *Chem Eng Sci.* 2002;57:4865–4876.
- Blok JR, Drinkenburg AAH. Hydrodynamics and mass-transfer in pulsing trickle-bed columns. *ACS Symp Ser.* 1982;196:393–406.
- Castellari AT, Haure PM. Experimental-study of the periodic operation of a trickle-bed reactor. *AIChE J.* 1995;41:1593–1597.
- Khadilkar MR, Al-Dahhan MH, Dudukovic MP. Parametric study of unsteady-state flow modulation in trickle-bed reactors. *Chem Eng Sci.* 1999;54:2585–2595.
- Nijhuis TA, Dautzenberg FM, Moulijn JA. Modeling of monolithic and trickle-bed reactors for the hydrogenation of styrene. *Chem Eng Sci.* 2003;58:1113–1124.
- Lebens PJM, Stork MM, Kapteijn F, Sie ST, Moulijn JA. Hydrodynamics and mass transfer issues in a countercurrent gas-liquid internally finned monolith reactor. *Chem Eng Sci.* 1999;54:2381–2389.
- Smits HA, Stankiewicz A, Glasz WC, Fogl THA, Moulijn JA. Selective three-phase hydrogenation of unsaturated hydrocarbons in a monolithic reactor. *Chem Eng Sci.* 1996;51:3019–3025.
- Nijhuis TA, Kreutzer MT, Romijn ACJ, Kapteijn F, Moulijn JA. Monolithic catalysts as efficient three-phase reactors. *Chem Eng Sci.* 2001;56:823–829.
- Kreutzer MT, Du P, Heiszwolf JJ, Kapteijn F, Moulijn JA. Mass transfer characteristics of three-phase monolith reactors. *Chem Eng Sci.* 2001;56:6015–6023.
- Heibel AK, Vergeldt FJ, Van As H. Gas and liquid distribution in the monolith film flow reactor. *AIChE J.* 2003;49:3007–3017.
- Mudalamane R, Bigio DI. Process variations and the transient behavior of extruders. *AIChE J.* 2003;49:3150–3160.
- Nijhuis TA, Beers AEW, Vergunst T, Hoek I, Kapteijn F, Moulijn JA. Preparation of monolithic catalysts. *Cat Rev Sci Eng.* 2001;43:345–380.
- Brandrup J, Immergut EH, Grulke EA, Bloch D. *Polymer Handbook*. New York: John Wiley and Sons, 1999:VII, 23.
- Triplett KA, Ghiaasiaan SM, Bdel-Khalik SI, Sadowski DL. Gas-liquid two-phase flow in microchannels—Part I: two-phase flow patterns. *Int J Multiphase Flow.* 1999;25:377–394.
- Snijder ED, Versteeg GF, Van Swaaij WPM. Some Properties of Lani5-Xalx metal-alloys and the diffusion-coefficient and solubility of hydrogen in cyclohexane. *J Chem Eng Data.* 1994;39:405–408.
- Fogler HS. *Elements of Chemical Reaction Engineering*. Upper-Saddle River, NJ: Prentice Hall, 1999:758–759.
- Wilke CR, Chang P. Correlation of diffusion coefficients in dilute solutions. *AIChE J.* 1955;1:264–270.
- Bercic G, Pintar A. The role of gas bubbles and liquid slug lengths on mass transport in the Taylor flow through capillaries. *Chem Eng Sci.* 1997;52:3709–3719.
- Cybulski A, Stankiewicz A, Albers RKE, Moulijn JA. Monolithic reactors for fine chemicals industries: a comparative analysis of a monolithic reactor and a mechanically agitated slurry reactor. *Chem Eng Sci.* 1999;54:2351–2358.
- Winterbottom M, Marwan H, Natividad R. Selectivity, hydrodynamics and solvent effects in a monolith cocurrent downflow contactor (CDC) reactor. *Can J Chem Eng.* 2003;81:838–845.
- Pandit AB, Rielly CD, Niranjana K, Davidson JF. The convex bladed mixed flow impeller—a multipurpose agitator. *Chem Eng Sci.* 1989;44:2463–2474.
- Waghmare Y, Knopf FC, Rice RG. The Bjerknes effect: explaining pulsed-flow behavior in bubble columns. *AIChE J.* 2007;53:1678–1686.
- Liu GZ, Duan Y, Wang YQ, Wang L, Mi ZT. Periodically operated trickle-bed reactor for EAQs hydrogenation: experiments and modeling. *Chem Eng Sci.* 2005;60:6270–6278.
- Haure PM, Hudgins RR, Silveston PL. Periodic operation of a trickle-bed reactor. *AIChE J.* 1989;35:1437–1444.
- Knopf FC, Waghmare Y, Ma J, Rice RG. Pulsing to improve bubble column performance. II. Jetting gas rates. *AIChE J.* 2006;52:1116–1126.
- Benjamin TB, Ursell F. The stability of the plane free surface of a liquid in vertical periodic motion. *Proc R Soc Lond Ser A* 1954;225:505–515.

Manuscript received Aug. 23, 2007, and revision received Dec. 21, 2007.